Corona Wind Visualization in an Asymmetric Capacitor using Liquid Nitrogen

Adrian Ieta[1], Zachariah Schrecengost[1], Marius Chirita*[2], and Jacob Mills[1]
[1]Dept. of Physics
SUNY Oswego University
phone: (1) 315-312-6394
e-mail: adrian.ieta@oswego.edu
[2]National Institute for Research and Development in Electrochemistry and Condensed Matter, Romania
*Author to whom any correspondence should be addressed.

***Abstract*— Applying high voltage to an electrode system generates a high electric field. Above the onset voltage corona current is generated. The ionization area is restricted near the stressed electrode but ions migrate imparting part of momentum to the nearby neutral molecules and creating the corona wind. A visualization technique of the corona wind is presented for a commonly used configuration (asymmetric capacitor) in electrohydrodynamic (EHD) lifters which employ the wind momentum for propulsion. The technique makes use of the vapors naturally occurring in air, condensed by means of temperature cooling by liquid nitrogen. The flow cross-sections are obtained by light scattering on the water vapors using a 10^{o} fan angle laser sheet. The method has the advantage of not introducing additional particles such as smoke particles for the purpose of flow visualization. The obtained profiles are relevant to the analysis of the lifter propulsion and electrostatic flow control in general.**

I. INTRODUCTION

Using high voltage across a thin wire allows for the surrounding air to start carrying ions; while traveling through the air the ions impart momentum to neutral molecules, motion that is macroscopically observable – the corona or ionic wind (first observed in 1709 as reported by Robinson [1]). The energy of the electric field is in this case partly converted to kinetic energy of the air flow. The speed of the flow was found experimentally [2, 3] and theoretically [3] to be proportional to the corona current. If used properly, it can be conducive to having the entire device fly in the air [4-8]. This levitation phenomenon is called the Brown-Biefeld effect after the scientists who discovered it (see patent [9]). The ionic wind can be generated in a positive or negative polarity as well as in ac coronas. Negative corona does not produce as much corona wind as positive corona [7, 10]. The wind can reach several m/s and it was reported to even reach 10 m/s if optimized [11]. The airflow can also be optimized by this method [12].

In corona discharges, diffusion is considered to play a minor role in the ion flow. The magnetic effects produced by corona currents are also ignored for simulations. The unipolar space charge flow of single-mobility ion species is governed by a set of equations subject to boundary conditions:

$$\nabla^2\Phi = -\frac{\rho}{\varepsilon}; \qquad \nabla\cdot(\rho\nabla) = 0 \tag{1}$$

where Φ is the voltage potential ρ is the charge density and ε is the dielectric permittivity. For corona wind simulations, the equations are coupled with Navier-Stokes equation and continuity equation:

$$\frac{\partial\vec{v}}{\partial t} + (\vec{v}\cdot\nabla)\vec{v} = \frac{1}{\rho_{air}}\vec{F} - \frac{1}{\rho_{air}}(\nabla p) + v\nabla^2\vec{v}\cdot = 0 \tag{2}$$

and continuity equation

$$\nabla\cdot\vec{v} = 0 \tag{3}$$

where $\vec{v}$ is velocity, *v* is the kinematic viscosity of the air, ρ_{air} is the density of the air, $\vec{F}$ is the electric force in this case, and *p* is air pressure. It is assumed that the fluid (air) is incompressible and it has constant viscosity and density.

The ionic wind allows for the manipulation of the airflow around profiles [13]. There are other significant engineering applications such in electrostatic cooling [14], electrostatic precipitation, electro-fluid-dynamic actuators [15], aeronautics (airflow control around a plane wing) [15, 16] and combustion control [17].

Since the invention of lasers new airflow visualizations and measurement methods have been developed [18]. Visualization of the corona wind is important and it was performed using various methods. A laser sheet and light scattering on smoke particles have been used for visualization of airflow around corona wire [2, 19]; Schlieren optical visualization has also been applied to ionic wind [20]. Laser induced phosphorescence [21] also revealed the corona wind. Numerical simulations [5, 10, 22] and theoretical calculations based on well justified use of Deutsch assumptions [7] were of great help in understanding the experimental work in the field. Nevertheless, corona wind visualizations that actually show the fluid flow induced are rather few and may require expensive equipment. Schlieren visualization converts the air density variations into a gray scale and it works well at large air speeds as there is a larger pressure gradient in the flow. Laser induced phosphorescence [21] makes use of additional biacetyl tracer vapors which may also change the ionic properties [20]. Using smoke in conjunction with a laser sheet can recover cross-sections in the flow [2, 19] but the smoke itself may interfere with the corona discharge process. Similarly for other methods using microparticles, or dye in the flow.

We report here an experimental study for corona wind visualization using water vapor condensation (naturally occurring in the air), induced by low temperature of the liquid nitrogen surrounding the corona wind generator. Corona wind profiles are generated in a simple fashion using a 10^o fan angle green laser sheet.

II. Experimental Setup and Procedure

A. Asymmetric Capacitor

An asymmetric capacitor was built from Balsa wood, aluminum foil (20 cm wide, 5 cm height), and thin steel wire of 0.160 mm diameter (34 gauges) as shown in Fig. 1. The apparatus is set to a vertical position on an additional balsa wood horizontal base.

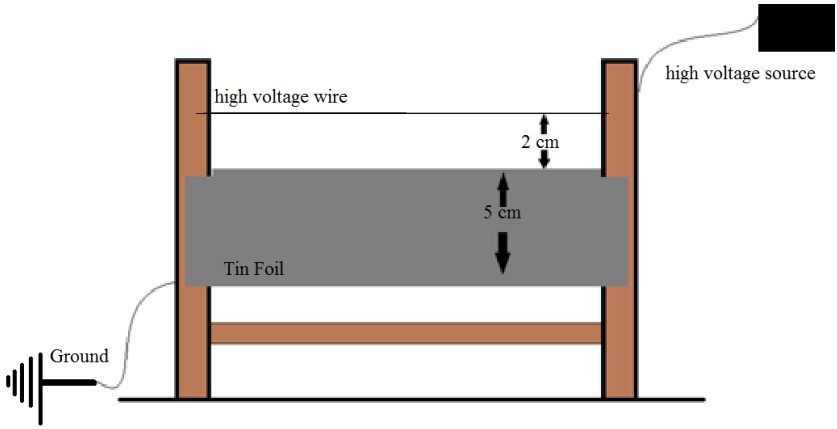

Fig. 1. Schematics of the apparatus (asymmetric capacitor).

A 2-cm separation between the high voltage wire and the aluminum foil was used in our experiments. The thin wire (corona wire) was hooked to the high voltage power supply with a positive polarity (Spellman HVPS +40kV DC) while the aluminum foil was grounded. The apparatus in Fig. 1 is an essential building block of electrostatic lifters such as the one in Fig. 5. Although the corona wind generated is pointing downwards, due to the wind hitting the horizontal apparatus base, the overall momentum imparted to the device is zero unlike in the case of lifters.

B. Corona wind visualization

Naturally occurring water vapors are used for corona wind visualization. Although the temperature of liquid nitrogen is very low (boiling point -196^{o}C), it does not decrease the temperature of the environment by much, as it is well known that liquid nitrogen is a very inefficient coolant. The presence of additional nitrogen in air (already made up of more than 75% nitrogen) does not influence its properties significantly (positive nitrogen ions are the most significant ion species in a positive wire plate-corona in air [23]).

A laser sheet (LBS-532-TL-80-10 Brightline Pro 532nm, 80mW) with a 10 degree fan angle was used to obtain light scattering cross-sections in the generated water vapors around the corona wind. Liquid nitrogen was loaded into six Erlenmeyer flasks, approximately 30 cm away and aligned with the apparatus. The setup was performed in a dark laboratory room in order to enhance the visualization effect.

Positive high voltage was applied to the wire on voltages ranging from zero up to +20 kV (air breakdown would usually occur around this voltage). The visualizations were photographed and video recorded.

In addition, electrostatic lifters were built from balsa wood and levitated (Fig. 5). Their masses ranged between 5 g and 10 g. The levitation was achieved within the 17 kV to 27 kV range. The generated lifting force is approximated by the formula found in empirical studies and also derived from fundamental principles as shown in recent theoretical work [7]:

$$F = I\frac{ka}{\mu} \tag{4}$$

where "I" is the corona current, "a" is the distance between the corona wire and the ground electrode, "k" is a constant of proportionality, while μ is the average mobility of ions. Visualization of the corona wind for the lifter was performed using the same procedure described above.

III. Analysis

Fig. 2 shows the visualizations of water vapor flow through and over the corona wind apparatus. Guiding tubes for the evaporating liquid nitrogen were attached to two Erlenmeyer flasks.

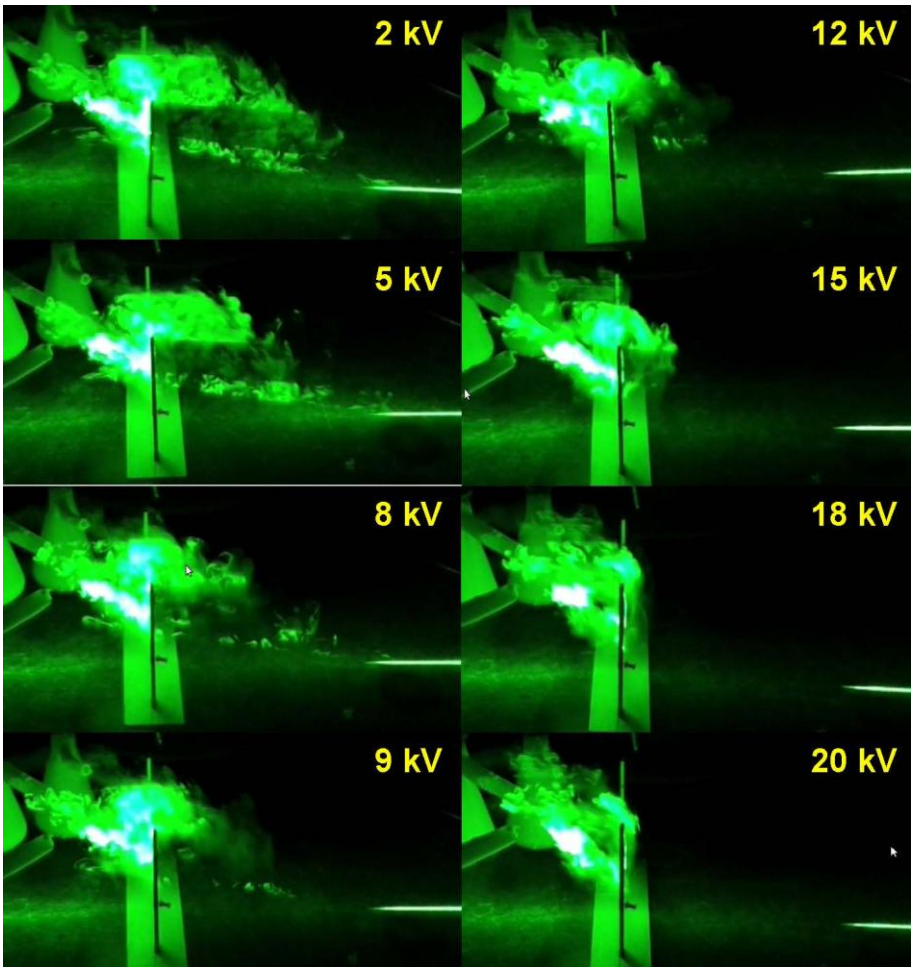

Fig. 2. Flow visualization: vertical cross-section of the turbulent flow of water vapors across the corona wind apparatus (laser light comes from the left and it is reflected back by a plane mirror on the right).

The laser sheet is projected from the right in a plane perpendicular to the wire. An additional plane mirror reflects the laser light within the same cross-section of the incident light. It also creates a reference line visible on the right hand side of each photo. The flow of vapors is not significantly different between 0 and 5 kV. Although the flow is more confined to the apparatus at 8 kV, significant changes and adherence to the apparatus are noticed at 9 kV and they grow in intensity at higher voltages. Between 18 kV and 20 kV the water vapors jet is almost completely confined by the proximity of the apparatus.

A different vapor insertion was performed for the visualizations in Fig. 3. The liquid nitrogen flasks are symmetrically arranged on both sides of the apparatus and no tubes are attached to them. The vapors spread out in a reasonably uniform fashion. The laser sheet is projected in a horizontal plane and in the direction of the apparatus axis and it points at the lower side of the ground electrode. Increasing the voltage progressively up to 8 kV shows very little changes (hardly noticeable) in the light scattering patterns. However, the transition to 9 kV clearly produces significant changes. At 12 kV hardly any vapors are present on the plane of the laser sheet as they are dragged away by the ionic wind. This status remains the same at larger voltages.

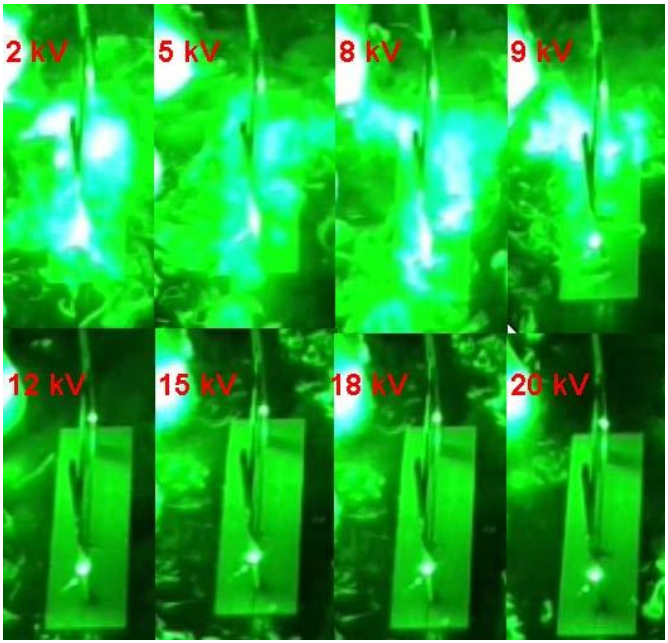

Fig. 3. Flow visualization: horizontal cross-section in the vertically generated ionic wind. The laser sheet is parallel to the base of the apparatus and at the lower level of the ground electrode.

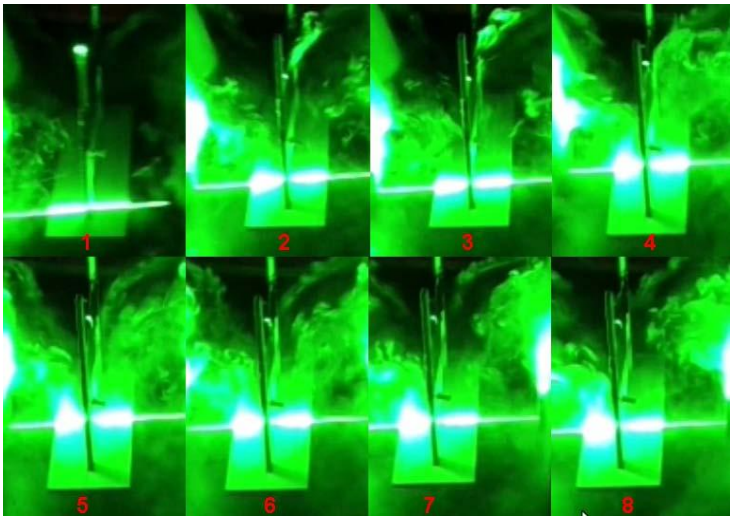

Fig. 4. Flow visualization: turbulent flow development in the corona wind. The image sequence was recorded within less than 1 second at 16.5 kV; the laser light comes vertically and perpendicular to the apparatus.

Fig. 4 shows the development of the water vapor flow induced by the ionic wind at 16.5 kV in an arrangement similar to the one described for characterization purposes in Fig. 3. The eight image sequence is recorded within less than (but close to) a second. The laser sheet points from above perpendicular to the high-voltage wire, generating a cross-section pattern of the ionic wind flow. The external water vapors are clearly absorbed into the corona wind stream.

Fig. 5 shows a levitating electrostatic lifter. The corona wind is visualized by the scattered light of the water vapors. It is noticeable that little wind influence is observed at low voltages (but higher than the corona onset). The transition to significantly identifiable wind is observed within narrow voltage ranges (less than a kV).

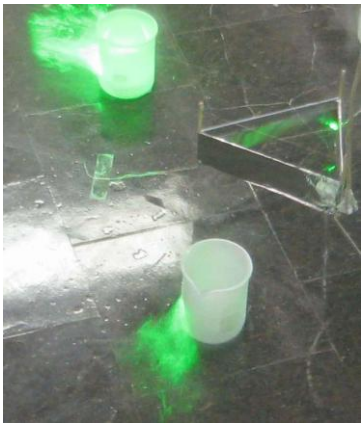

Fig. 5. Flow visualization for a flying electrostatic lifter.

IV. Conclusion

The applicability of liquid nitrogen generated water vapor condensation in the visualization of the corona wind has been experimentally demonstrated. While the effectiveness of the method is apparent, the influence of the water vapors produced by liquid nitrogen has yet to be explored in more details. Vapor distribution is essential for obtaining the light scattering profiles to be seen using a laser sheet. The procedure allows for the optimization of water vapor generation in conjunction with the corona wind generator configuration. Our study showed that corona wind, although present at voltages above corona onset, becomes significant only when the voltage exceeds certain levels (in our case the transition was significant while voltage was increased from 8 to 9 kV).

V. Acknowledgements

The work was sponsored in part by the Summer Science Immersion Program at SUNY Oswego and a college SCAC grant. The authors are thankful to Gabriella Medina, Tajia-Rae Thurston, Christopher Wahl, and Bruce Zellar for helping with the project.

References

[1] Robinson, M. "A History of the Electric Wind." *American Journal of Physics* 30.5 (1962): 366–372.
[2] Moreau, E., Leger, L., and Touchard, G. "Effect of a DC surface-corona discharge on a flat plate boundary layer for air flow velocity up to 25 m/s." *Journal of Electrostatics* 64 (2006): 215-225.
[3] Go, D. B., Maturana, R. A., Fisher, T. S., Garimella, S. V. "Enhancement of external forced convection by ionic wind." *International Journal of Heat and Mass Transfer* 51 (2008): 6047-6053.
[4] Koziell, L.; Zhao, L., Liaw, J., Adamiak, K. "Experimental Studies of EHD Lifters." *Proc. ESA Annual Meeting on Electrostatics 2011*.
[5] Zhao, L., Adamiak, K. "Numerical analysis of forces in an electrostatic levitation unit." *Journal of Electrostatics* 63 (2005): 729–734.
[6] Bahder, T., Fazi, C. "Force on an Asymmetric Capacitor." Army Research Laboratory Tech Report No. ARL-TR-3005, March 2003.
[7] Ianconescu, R., Sohar, D., and Mudrik, M.. "An Analysis of the Brown-Biefeld Effect." *Journal of Electrostatics* 69 (2011): 512-521.
[8] Tajmar, M. "Biefeld-Brown Effect: Misinterpretation of Corona Wind Phenomena." *AIAA Journal* 42.2 (2004): 315-318.
[9] T.T. Brown, "A method of and an apparatus or machine for producing force or motion", BP 300311, (1928).
[10] Martins, A. A., and Pinheiro, M. J. "On the nature of the propulsive force of asymmetric capacitors in the atmosphere." *Physics Procedia* 20 (2011): 103-111.
[11] E. Moreau, G. Touchard. "Enhancing the mechanical efficiency of electric wind in corona discharge." *Journal of Electrostatics* 66 (2008): 39-44.
[12] Rickard, M., Dunn-Rankin, D., Weinberg, F., and Carleton, F. "Maximizing ion-driven gas flows." *Journal of Electrostatics* 64.6 (2006): 368–376.
[13] Moreau, E. "Airflow control by non-thermal plasma actuators." *Journal of Physics D: Applied Physics* vol. 40 (2007): 605-636.
[14] Go, D. B., Garimella, S. V., Mongia, K. R., and Fisher, T. S. "Ionic winds for locally enhanced cooling." *Journal of Applied Physics* 102 (2007): 053302.
[15] Moreau, E., Sosa, R., and Artana, G. "Electric wind produced by surface plasma actuators: A new dielectric barrier discharge based on three-electrode geometry." *Journal of Physics D: Applied Physics* vol. 41.11 (2008): 115204.
[16] Mestiri, R., Hadaji, R., Nasrallah, S. B. "An experimental study of a corona discharge at the surface of an insulating material." *Heat and Technology* 27 (2009): 65-68.

[17] Carleton, F. B. and Weinberg, F. J. "Electric field-induced flame convection in the absence of gravity," *Nature* 330 (1987): 635 – 636.
[18] Prenel, J. P., Ambrosini, D. "Flow visualization and beyond." *Optics and Lasers in Engineering* 50.1 (2012): 1-7.
[19] Léger, L., Moreau, E., Artana, G., and Touchard, G. "Influence of a DC corona discharge on the airflow along an inclined flat plate." *Journal of Electrostatics* 51-52 (2001): 300-306.
[20] Ohyama, R., Inoue, K., and Chang, J. S. "Schlieren optical visualization for transient EHD induced flow in a stratified dielectric liquid under gas-phase ac corona discharges." *Journal of Physics D: Applied Physics* 40.2 (2008): 573.
[21] Ohyama, R., Aoyagi, K., Kitahara Y., and Ohkubo Y. "Visualization of the local ionic wind profile in a DC corona discharge field by laser-induced phosphorescence emission." *Journal of Visualization* 10.1 (2007): 75-82.
[22] Zhao, L., Adamiak, K. "EHD flow in air produced by electric corona discharge in pin–plate configuration." *Journal of Electrostatics* 63.3-4 (2005): 337–350.
[23] Chen, J., and Davidson, J. H. "Electron density and energy distributions in the positive DC corona: Interpretation for corona-enhanced chemical reactions." *Plasma Chemistry and Plasma Processing* 22.2 (2002): 199-224.